Astron. Astrophys. 274, 87–95 (1993)

ASTRONOMY AND ASTROPHYSICS

Kinematics of a sample of globular clusters in the halo and the mass of M 31

L. Federici[1], F. Bònoli[2], L. Ciotti[1,3], F. Fusi Pecci[1,2], B. Marano[1], V. A. Lipovetsky[4], S. I. Neizvestny[4], and N. Spassova[5]

[1] Osservatorio Astronomico, Via Zamboni 33, I-40126 Bologna, Italy
[2] Dipartimento di Astronomia, Univ. Bologna, CP 596, I-40100 Bologna, Italy
[3] Princeton University Obs., Peyton Hall, Princeton, NJ 08544, USA
[4] Special Astrophysical Observatory, USSR
[5] Department of Astronomy, Bulgarian Academy of Sciences, Sofia, Bulgaria

Received July 18, 1992; accepted March 2, 1993

Abstract. New spectroscopic observations of 35 M 31 globular cluster candidates, located at galactocentric distances larger than 10 kpc from the nucleus of the galaxy, have been carried out in two different runs at the 6m *BTA* telescope. Radial velocities for 21 new confirmed clusters never observed so far are presented.

After these observations, all the high confidence cluster candidates located farther than 13 kpc from the M 31 nucleus have been spectroscopically checked and 29 have been confirmed to be globular clusters.

Adding these new data to all published cluster radial velocities, the total sample of spectroscopically confirmed M 31 globular clusters includes 176 objects, with typical velocity errors ≤ 30 km s^{-1}.

Two different approaches applied to the global sample to get hints on the galaxy total mass give some indications favouring a possible steady increase of the M 31 mass up to values typical for a massive halo ($\sim$ 5–8 $\times 10^{11} M_{\odot}$, at 30 kpc), but the assumptions imposed by the methods in absence of a firm knowledge of the actual orbit distribution severely limits the reliability of this result.

Key words: galaxies: individual – M 31 – galaxies: fundamental parameters – galaxies: kinematics and dynamics – galaxies: star clusters – dark matter

1. Introduction

In the latest years, a wide effort has been undertaken to have a better insight into the shape of the mass distribution in galaxies. It is also well known that the study of the kinematics of the globular cluster systems in external galaxies can give important information on this issue. In fact, globular clusters can be used as test particles for examining the mass distribution of the parent galaxy via conventional mass estimators and comparisons with models, getting also an estimate of its total mass (see Federici et al. 1990, hereafter *Paper I*, and references therein).

We are currently involved in a long-term project (started in 1976) for studying the cluster system of M 31. The strongest effort has been devoted until recently to the very difficult search for reliable candidates (Battistini et al. 1980, 1987, 1993). We have also started some preliminary analyses of their intrinsic properties (Cacciari et al. 1982; Buonanno et al. 1982; Battistini et al. 1982; Bònoli et al. 1987, 1988, 1992; Crotts et al. 1990), and a study of their kinematics (*Paper I*). A global revision and discussion of all the available data is in progress (Battistini et al. 1993, in preparation). Here we present the results obtained in a further step made carrying out spectral observations of a sample of cluster candidates, mostly in the outer halo.

First systematic spectroscopic observations of a sample of globular clusters in M 31 were made in 1969 by van den Bergh. References to further observations and discussions can be found in Kent et al. (1989, hereafter *KHS*), Peterson (1989), and in *Paper I*.

Using a sample of 81 spectroscopically observed clusters, we were able to point out in *Paper I* some interesting considerations and conclusions. First, we found that a "straight" application of conventional mass estimators (like the Projected Mass [PM] method) to the whole cluster population leads to "artificial" agreement with other mass determinations, mainly because it fails in assigning proper weight to the kinematical information coming from different projected radii. Hence, we put some cautions on the adoption of the value of $(3.1 \pm 0.5) \times 10^{11} M_{\odot}$ for the total mass of M 31 obtained via this procedure for instance by Huchra et al. (1991). Second, by applying the PM estimator to concentric shells in order to overcome somehow the problem, we got that existing data indicate a steady increase of the M 31 mass with radius, up to about $3.2 \times 10^{11} M_{\odot}$ at 16 kpc and, further, they are compatible with a steep increase at larger distances. Third, by comparing observations with a set of models computed by Richstone & Tremaine (1984), we noticed that

Send offprint requests to: L. Federici

© European Southern Observatory • Provided by the NASA Astrophysics Data System

(i) only circular or isotropic orbits are compatible, and (ii) the best fitting model, based on circular orbits, leads to an effective radius of 22^{-9}_{+16} kpc and a total mass of about $7^{-3}_{+7} \times 10^{11} M_{\odot}$. The validity of this approach has been recently convincingly questioned by S.M. Kent (the Referee of the present paper) and we re-examine here the problem making use of a different procedure, besides of a larger data-set.

At the same time, the availability of the new spectroscopic data secured at the *CfA*, led Kent, Huchra and Stauffer (*KHS*) to investigate the shape of the mass distribution in M 31 from the motions of its globular clusters and the use of a three-component mass model for M 31 developed by Kent (1987, 1989). These Authors conclude that *with no assumptions about the isotropy of the velocity distribution, the globular cluster kinematics are consistent with the mass distribution inferred from the rotation curve* but *if the velocity distribution is globally isotropic, then the relatively low rotation velocity of the globular cluster system is inconsistent with a model in which all of the mass lies in a spherically symmetric halo.* Moreover, *if the velocity distribution is locally isotropic, then the approximate constancy of the projected second moment with radius also rules out a model that lack a massive halo.*

It is quite evident the difficulty to draw any firm conclusion and both groups stress that only further observations of radial velocities for a wider sample of distant globular clusters can yield a better understanding of the mass distribution in M 31.

Since our survey has produced new cluster candidates at large distance from the M 31 bulge, we decided to carry on specific spectroscopic observations at the Zelenchuk 6m telescope (*Bolshoi Alt-azimuth Telescope, BTA*) of the Special Astrophysical Observatory (*SAO*) of the USSR Academy of Sciences, within the frame of a cooperation involving the Italian CNR and the Academies of Sciences in USSR and Bulgaria.

In this paper, we present the radial velocities we obtained for 35 clusters (21 never measured so far) in the outer halo of M 31 and some considerations we inferred on the M 31 mass from the motions of these outer clusters merging them into the sample of all previously published data.

2. Observations and reductions

2.1. Selection of the objects

In the preparation of the list we choose to use (as described in *Paper I*, Sect. 2.1) a relatively loose selection criterion in order to be sure that all clusters could be included and also to check the actual nature of the typical contaminating objects. Distant compact galaxies are obviously expected to be the principal spurious candidates, increasing in percentage in the outer regions of M 31, where the surface density of globular clusters drops off quite rapidly. Fortunately enough, since only a few confirmed M 31 clusters have intrinsic colours (B–V)>1 in the regions outside the main body of M 31 where "internal" reddening is negligible (see Battistini et al. 1993), a red colour index most often indicates that the candidate is actually a galaxy. On the other hand, the opposite is not true. As a matter of fact, a number of galaxies with (B–V)<1 are undistinguishable from M 31 globular clusters in ordinary images. However, during acquisition we could interrupt in real time the integration (see Sect. 2.2) as soon as clear galaxian features were observed, thus saving a significant amount of observing time.

We adopted as reference list the catalogues presented by Battistini et al. (1987, hereafter *BoSurvey*). We selected from *BoSurvey* Table IV (*Globular cluster candidates: A and B classes*) all candidates never observed spectroscopically and having projected galactocentric distances larger than 50 arcmin ($\sim$ 10 kpc). We added then to this sample the objects from *BoSurvey* Table VII taken from the Sargent et al. (1977) catalogue (*out of field* candidates) which were inspected and classified on good Tautenburg Schmidt plates (V and I) by two of us (F.B. and F.F.P.) during a stage at Tautenburg Observatorium (Germany). To convert angular distances, we adopted for M 31 a distance modulus $(m - M)_o = 24.12$, which corresponds to a linear distance of $\sim$ 667 kpc (Sandage & Tamman 1971).

Finally, a number of already observed globular clusters were added to the list as velocity standards.

2.2. Observations

Observations were performed with the 6m BTA telescope at the Nasmyth focus (F/30), in 4 half nights on September 1989 and 3 half nights on September 1990. We used the spectrophotometer (1-D scanner) mounted on the modified diffraction spectrograph SP-124 (Somova et al. 1982). The spectrophotometer scans two lines with 1024 channels each (one for object and one for sky). It is an almost classical image photon counting system (IPCS) of the Boksenberg (1972) type: 4-stage EMI magnetically focused image tube with S20 photocathode, lens coupling to a TV scanner, on-line background rejection and photon centroid computation.

We used a 600 lines/mm grating, giving in the spectral range 3700-5600 Å a 1.9 Å channel^{-1} dispersion with a 2.5 arcsec diaphragm. With this set-up, the FWHM of unblended lines of the comparison lamp is about 7-8 Å. Exposure times ranged between 10 and 40 min.

The apparatus permits to obtain simultaneous photometry of the object observed with the spectrograph, using a beam splitter. In particular, there are the following possibilities of simultaneous observations (spectroscopy + photometry):

i) multicolour photometry (e.g. *UBVR* Johnson system);

ii) the light curve in one filter with time resolution 0.001-1 sec (with or without background subtraction):

iii) high speed photometry with time resolution till 1 μsec (recording time of each photon);

Acquisition, control and monitoring are made with a Soviet analog of the computer *PDP-11*.

2.3. Reductions

The reduction procedures were quite similar to those described in *Paper I*. The first steps of reductions (i.e.: division by a quartz

© European Southern Observatory • Provided by the NASA Astrophysics Data System

lamp exposure, wavelength calibration referred to the two nearest comparison spectra, and sky subtraction) were performed in Bologna using the *Munich Image Data Analysis System* (MIDAS) package. A cross–correlation technique with a template spectrum, as developed by Pier (1983) and modified by us (*Paper I*), was then applied to measure radial velocities.

Following the experience gained in our previous work (see *Paper I*), we chose to adopt as template spectrum the sum of the spectra of the clusters in common with *KHS*, shifted to $v_r = -301$ km s^{-1}, the adopted radial velocity of the center of mass of M 31 (Yahil et al. 1977). All our spectra have then been cross–correlated with this "artificial" high signal–to–noise globular cluster spectrum. Table 1a presents the list of objects observed at the 6m BTA and the obtained heliocentric velocities. Clusters used to build up the template are marked with an asterisk.

During observations at SAO, the bright M 31 cluster *Bo 225* was observed each night, in order to have a check of the reliability of our results. The mean of the 6 values we obtained for the radial velocity of *Bo 225* is $<v>= -167 \pm 26$ km s^{-1}.

2.4. The global sample

Since in the following analysis and discussion we want to use a sample of clusters as large as possible made by adding radial velocities for the objects observed at SAO to the other published values, we preliminarily checked the consistency of the velocity measurements carried out in all the various considered studies. We have therefore recalibrated all the velocities presented in *Paper I* using the new velocities from *KHS*, which are slightly different from those published by Huchra et al. (1982) and adopted in *Paper I* to build up the template (these new values are listed in Table 1b).

Total errors affecting the adopted velocities can be estimated by comparing *KHS*, *Paper I–recalibrated* and the present results for the clusters in common. This comparison gives:

$< v_{ours} - v_{KHS} >= -1.3 \pm 23.0 km\ s^{-1}$;

$< v_{ours} - v_{Paper I(recalib.)} >= -1.5 \pm 11.8 km\ s^{-1}$.

Since typical errors for velocities given by *KHS* are ≈ 30 km s^{-1}, our new values should be affected by a similar or smaller error. Moreover, having adopted after recalibration also the same *zero–point*, the data on radial velocities of M 31 globular clusters can be considered to be homogeneous. Henceforth, we will use this *Global Sample* as a unique set in the following discussion. The Global Sample so obtained provides the best homogeneous sample of velocities for 176 globular clusters in M 31 (Fig. 1). Further, as thoroughly discussed in Battistini et al. (1993), it is also surely sufficiently representative of the whole cluster population down to V $\sim$ 18 and out to 20 kpc from the M 31 nucleus, though it is still not complete.

3. Implications for total mass and mass distribution of M 31

The determination of the shape of the mass distribution in galaxies and of their total mass still represents one of the most difficult goal to accomplish even for the members of the Local Group.

Table 1a. List of cluster names, adopted velocities, and distances for the clusters observed at SAO 6m BTA

Bo	G	Distance (arcm)	Distance (kpc)	Velocity‡ (km s^{-1})
19	72	21.15	4.1	-223.1 (2) *
23	78	19.55	3.8	-423.7 (2) *
34	96	26.56	5.2	-524.3 (2) *
144		2.89	0.6	-246.5 (1)
163	217	13.18	2.6	-167.8 (2) *
193	244	23.67	4.6	-46.4 (1) *
225	280	20.51	4.0	-166.9 (6) *
295	14	88.18	17.1	-363.2 (1) *
290		95.29	18.5	-381.3 (1)
301	22	88.05	17.1	-418.9 (1)
304	28	43.17	8.4	-304.9 (1)
306	29	58.40	11.3	-415.3 (1) *
309	31	72.36	14.0	-479.8 (1)
315	38	55.66	10.8	-434.1 (1) ◇
325		52.66	10.2	-560.2 (1)
327	53	47.81	9.3	-569.2 (1)
337	68	60.08	11.7	-232.3 (1)
339	77	82.66	16.0	-188.0 (1)
341	81	44.11	8.6	-272.5 (1)
345	143	58.81	11.4	-293.2 (1)
350	162	51.41	10.0	-251.7 (1)
356	206	34.72	6.7	-49.5 (1)
357	209	65.46	12.7	-271.7 (1)
361	255	63.62	12.3	-329.5 (1)
365	284	64.67	12.6	72.3 (1)
366	291	52.88	10.3	-173.1 (1) *
372	304	54.37	10.6	-195.5 (1) *
383	318	39.14	7.6	-272.7 (1)
392	329	61.53	11.9	98.2 (1)
401	344	65.48	12.7	-347.6 (1)
402	346	79.85	15.5	-487.6 (1)
	1	152.50	29.6	-334.8 (2) *
	3	110.83	21.5	-87.3 (2) †
	260	79.82	15.5	16.1 (1)
	353	116.05	22.5	-294.6 (1)

‡ in parentheses the number of the observations
* objects used as template
◇ this object has a spectral type much earlier than any of the template spectra
† G3 Huchra et al. (1991): galaxy+star
Bo Battistini et al. (1987)
G Sargent et al. (1977)

Table 1b. Radial velocities for clusters observed at 4m KPNO (from Federici et al. 1990), recalibrated as described in Sect. 2.4

Bo	G	Distance (arcm)	Distance (kpc)	Velocity‡ (km s^{-1})
19	72	21.15	4.1	-244.4 (1) *
23	78	19.55	3.8	-422.5 (1) *
27	87	26.43	5.1	-248.7 (1) *
34	96	26.56	5.6	-579.1 (1) *
158	213	10.46	2.0	-215.2 (1) *
163	217	13.18	2.6	-159.0 (1) *
193	244	23.67	4.6	-96.4 (1) *
201	250	14.30	2.8	-728.9 (1) *
212	263	18.58	3.6	-340.9 (1) *
213	264	20.75	4.0	-535.6 (1)
218	272	17.20	3.3	-243.5 (1) *
225	280	20.51	4.0	-160.5 (6) *
289		99.46	19.3	-180.5 (1)
291	9	87.71	17.0	-215.4 (1)
292	10	75.18	14.6	-265.4 (1)
293	11	75.75	14.7	-467.1 (1)
343	105	64.83	12.6	-359.5 (1)
358	219	87.17	16.9	-220.2 (1)
396	335	76.07	14.8	-561.3 (1)
400	343	91.11	17.7	-290.4 (1)
405	351	79.03	15.3	-106.4 (1)
407	352	87.08	16.9	-318.5 (1)
409		89.21	17.3	-53.6 (1) †
	1	152.50	29.6	-337.2 (1) *
	2	148.32	28.8	-231.5 (1)
	268	92.18	17.9	-320.8 (1) †
	327	99.64	19.3	-198.2 (1)
	339	126.47	24.5	32.7 (1)
	355	127.60	24.8	-59.5 (1) †
EX8		19.39	23.2	-154.1 (1)

‡ in parentheses the number of the observations
* objects used as template
† G3 Huchra et al. (1991): galaxy+star
Bo409 Sharov et al. (1989): stellar; Racine (1991): galaxy
G268 Racine (1991): galaxy
G355 Huchra et al. (1991): extended at MMT;
Racine (1991): star+galaxy
Bo Battistini et al. (1987)
G Sargent et al. (1977)

In particular, the measure of the relative subdivision between Bulge, Disk, and Halo may have an important impact on the hot issue of existence and nature of dark matter.

© European Southern Observatory • Provided by the NASA Astrophysics Data System

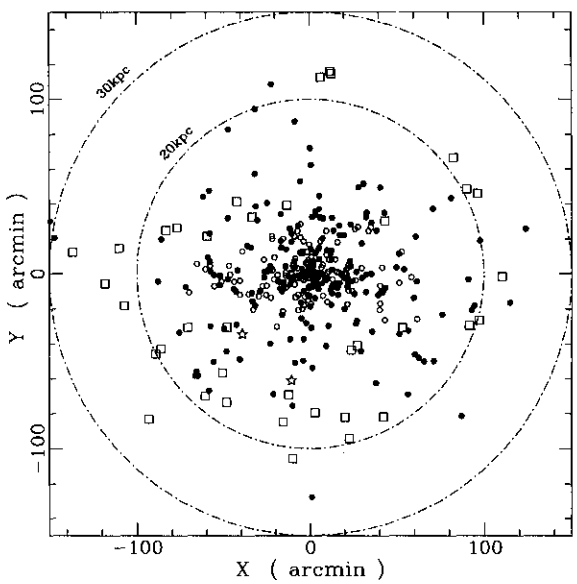

Fig. 1. Distribution of the M 31 globular clusters in X, Y coordinates referred to the center of the galaxy. At the adopted distance of M 31 (667 kpc) 100 arcmin correspond to 20 kpc; the plot covers an area around the galaxy of about 30 kpc in diameter. Squares indicate the candidates identified as galaxies and listed in Table 2, full dots indicate the 209 globular clusters, confirmed by spectroscopic observations and/or deep high-resolution imaging, and stars indicate the 4 candidates identified as stars. Finally, open dots mark the remaining 130 globular cluster candidates, not confirmed yet

Table 2. List of confirmed galaxies

Bo	G	References
140	196	R91
294	12	this paper, R91
296	15	HBK
297	16	this paper, HBK
299		this paper
300		this paper, R91
340		this paper, R91
360		R91
364		this paper, R91
369		this paper, R91
390		R91
394	331	HBK
395		R91
404	350	R91
406		this paper, R91
408	354	HBK
410		R91
421	19	R91
429	24	R91
434		R91
454	79	R91
455	80	R91
497	338	R91
498	340	R91
501	345	HBK, R91
509		R91
	4	Pap.I, HBK
	5	S84, Pap.I, CF, HBK
	6	this paper, CF, HBK
	7	S84, CF, HBK
	8	HBK
	145	HBK, CF
	171	this paper, R91
	225	Pap.I, HBK
	273	this paper, HBK
	294	Pap.I, HBK
	347	HBK
	349	HBK

Bo: Battistini et al. (1987) (BoSurvey)
CF: Cohen and Freeman (1991)
HBK: Huchra et al. (1991)
S84: Sitko (1984), Tab.2
G: Sargent et al. (1977)
Pap. I: Federici et al. (1990)
R91: Racine (1991)

Since globular clusters can be considered to be like test particles ruled by the parent galaxy mass distribution, the study of the kinematics of the cluster system could add important informations on this item. On the other hand, it is also true that it is very difficult to use the clusters as test particles without introducing some assumption about their orbital properties. In practice, it is almost impossible to obtain from them a direct and unique description of the mass shape of the parent galaxy, while it may be more viable to set constraints on the compatibilty between observations and possible galaxy models.

In the following paragraphs, we wish to measure the total mass of M 31 out to 30 kpc based on the kinematics of the globular clusters only and without reference to the rotation curve. We will follow two different approaches and anticipate that each of them is based on assumptions crucial to the method and not easy to verify. However, these experiments are in our view useful at least to point out the items requiring further observational and theoretical inputs. In particular, by applying the various procedures to both the *KHS* sample and the new one here presented (which differ essentially for the addition of our new external halo objects), we will show how important may be for the M 31 total mass determination the inclusion of new clusters located in the outer halo.

3.1. The two–component model

Schematically, this approach is based on the following steps:

a) We adopt a very simple dynamical model for M 31 consisting in just two spherically symmetric components, i.e. a bulge and a halo. Each component depends on some parameters (specifically here 2 for the halo and 1 for the bulge).

b) We compute the projected velocity dispersion for a system having the same projected density profile as that obtained from the observed clusters (Battistini et al. 1993), in the gravitational field of the bulge+halo system (i.e. the self–gravity of the globular cluster system is not considered). Moreover, we assume no overall rotation, and the description of the radial behaviour of the velocity dispersion tensor is determined from the Osipkov–Merritt formula (see e.g. Binney & Tremaine 1987, p. 240). This procedure will yield a further parameter describing the orbital anisotropy of the cluster system.

c) With the above special assumptions, we get then the parameters of the best fitting model by minimizing the sum of the squares of the residuals between the observed velocity dispersion and that computed from the adopted model.

We can start our analysis by adopting as reference an M 31 mass model similar to that used *KHS* (Model III), and repeat some of the computations they did essentially to verify whether we can get a consistent picture. Note that, though this may well be not the best model to use since no disk contribution is taken into account, it has the advantage of being simple and useful for our heuristic purposes. This procedure is convenient for the computation of spherically symmetric models, but one cannot directly compare the bulge and halo parameters with any model

© European Southern Observatory • Provided by the NASA Astrophysics Data System

that does include a disk esplicitly. Turning to the details, the model consists of the following components:

• A distribution of dark matter described by the quasi–isothermal law:

$$\rho_h(r) = \frac{\rho_{h0}}{1 + r^2/r_{ch}^2}. \quad (1)$$

So doing, the halo mass and its radial distribution are fully ruled by two quantities, i.e. the central density ρ_{h0} and the core radius r_{ch}. The mass inside the sphere of radius r is easily obtained by volume integration of Eq. (1):

$$M_h(r) = 4\pi\rho_{h0}r_{ch}^3[r/r_{ch} - ArcTan(r/r_{ch})]. \quad (2)$$

(note that the halo mass linearly diverges with the radius for $r \rightarrow \infty$).

• A bulge having the same geometric density distribution as adopted by Kent (1989), but with a dimensionless multiplicative coefficient,

$$\rho_b(r) = f_b \times \rho_{Kent}(r) \quad (3)$$

so that f_b is actually the third free parameter. We have also truncated the bulge at r = 3.5 kpc. Adopting $f_b = 1$, the total mass of the bulge turns out to be $2\times10^{10}M_\odot$, the value given by Kent (1989).

• The number density of the M 31 clusters, $n_{gc}(r)$, has then been taken from our latest analysis (Battistini et al. 1993) which yielded for the best fitting projected number density

$$\Sigma_{gc}(R) = \Sigma_0 exp[-b(m)(R/R_e)^{1/m}] \quad (4)$$

where $b(m) \simeq 2m - 0.324$ (Ciotti 1991), m = 1.6, R_e =4.59 kpc.

Once this simple model has been adopted, one can numerically solve the Jeans equation for the radial component of velocity dispersion, $\sigma_r^2(r)$:

$$\frac{dn_{gc}(r)\sigma_r^2(r)}{dr} + 2\frac{\beta(r)n_{gc}(r)\sigma_r^2(r)}{r} = - G\frac{[M_b(r) + M_h(r)]n_{gc}}{r^2}, \quad (5)$$

where $M_b(r)$ and $M_h(r)$ are respectively the mass of the halo and of the bulge, inside r.

We stress the fact that, since the cluster system is not self–gravitating, the mass term referred to the total cluster mass is lacking in the right part of Eq. (5). Consequently, the velocity dispersion is independent of Σ_0.

As usual $\beta(r)$ describes the radial trend of the orbital anisotropy of the globular clusters around the galaxy, and we adopt the functional form given by Merritt (1985):

$$\beta(r) = \frac{r^2}{r^2 + r_a^2}, \quad (6)$$

where r_a is a free parameter, called *anisotropy radius*, and that in our models assumes the values 0.0, 1.0, 10, 50, ∞. This parameter works in the sense that, for $r_a \rightarrow \infty$ $\beta = 0$ and the velocity dispersion is everywhere isotropic, whilst for $r_a = 0$, (i.e. $\beta = 1$), just radial orbits are obtained. Finally, for $r \leq r_a$ the distribution of the orbits is essentially isotropic, and $r \geq r_a$ the ellipsoid of the velocity dispersions is prolate (i.e. the orbits become radially anisotropic). With the assumption (6) for β, the solution of the Jeans equation (5) can be obtained in integral form (Binney 1980).

Having the radial component of the velocity dispersion we can now obtain the projected velocity dispersion, $\sigma_P(R)$, using then the well known relation (Binney & Mamon 1982):

$$\Sigma_{gc}^2(R)\sigma_P^2(R) = 2\int_R^\infty (1 - \frac{\beta(r)R^2}{r^2})\frac{n_{gc}(r)\sigma_r^2(r)rdr}{\sqrt{r^2 - R^2}}. \quad (7)$$

Again, the projected velocity dispersion is independent of Σ_0. In conclusion, the obtained locus depends on 4 parameters, i.e. $\rho_{h0}, f_b, r_{ch}, r_a$. Note also that the dependence on ρ_{h0} and f_b is linear:

$$\sigma_P^2(R) = \rho_{h0}\sigma_{Ph}^2(R; r_{ch}, r_a) + f_b\sigma_{Pb}^2(R; r_{ch}, r_a). \quad (8)$$

At this stage, knowing the observed velocity dispersion, it is possible to compute for each couple of (r_{ch}, r_a) values the quantity to minimize as a function of the other two (linear) parameters ρ_{h0} and f_b. As said, we use for this purpose the sum of the squares of the residuals between the observed velocity dispersion and the one predicted from the adopted model, taking into account appropriate weights based on the actual observational errors. As a consequence, the two scale–parameters can be explicitly obtained in algebric way, after differentiation of the estimator, thanks to the linearity of Eq. (8).

In practice, after choosing a couple of (r_{ch}, r_a) values, we have determined the corresponding figures for ρ_{h0} and f_b, and computed the estimator for the four fixed parameters. Then, by repeating the procedure for an appropriate grid of the input (r_{ch}, r_a) couple, we have determined the choice which yields the minimum value for the estimator. With all the caveats and limits connected to the procedure and assumptions, the resulting parameters define the "optimal" model deduced using the available data on individual cluster velocities. Moreover, the figure for r_a corresponding to the minimum of the adopted estimator, is also a quantitative index of the anisotropy of the cluster velocity dispersion.

We have explored the impact on the output parameters due to the variation of the law describing the cluster projected number profile and the data–sample. In particular, we present below some results obtained by applying the procedure described above to the two different samples considered here, i.e. first the sample adopted by *KHS*, and, second, the present sample. Note that, though the range in galactocentric distance covered by the whole sample is the same, we have essentially added a subset of 21 clusters in the outer bins, and this has a quite interesting impact on the results.

© European Southern Observatory • Provided by the NASA Astrophysics Data System

Table 3a. Best fitting solutions with the two-component models ($R^{1/4}$–law)

rebin	r_a (kpc)	r_{ch} (kpc)	ρ_{h0} ($M_\odot/pc^3$)	χ^2	$M_h^{(1)}$ ($10^{11}M_\odot$)	$M_h^{(2)}$ ($10^{11}M_\odot$)
R_e=8.32, f_b=1						
1	∞	1.5	0.69	3.02	4.42 (25)	5.39
2	50.	1.2	0.96	6.66	3.11 (20)	4.82
3	50.	1.2	0.95	1.04	2.58 (17)	4.84
R_e=5.34, f_b=1.						
1	∞	1.3	0.97	3.07	4.73 (25)	5.75
2	50.	1.1	1.22	6.71	3.41 (20)	5.27
3	∞	1.1	1.26	1.09	2.89 (17)	5.41
R_e=4.86, f_b=1.						
1	∞	1.3	0.99	3.08	4.82 (25)	5.86
2	50.	1.1	1.25	6.72	3.48 (20)	5.38
3	∞	1.1	1.28	1.09	2.95 (17)	5.51

(1) mass within the farthest bin, whose mean distance in kpc is in parentheses.
(2) mass within 30 kpc.

Table 3b. Best fitting solutions with the two-component models ($R^{1/m}$–law)

rebin	r_a (kpc)	r_{ch} (kpc)	ρ_{h0} ($M_\odot/pc^3$)	χ^2	$M_h^{(1)}$ ($10^{11}M_\odot$)	$M_h^{(2)}$ ($10^{11}M_\odot$)	M_b ($10^{11}M_\odot$)
R_{e0}=4.59, m=1.6, f_b=1.							
1	∞	4.0	0.19	3.66	7.38 (25)	9.25	2.0
2	50.	4.0	0.19	6.39	5.45 (20)	9.10	2.0
3	∞	3.5	0.22	1.30	4.11 (17)	8.52	2.0
R_{e0}=5.44, m=2.2, f_b=1.							
1	∞	2.5	0.34	3.53	5.63 (25)	6.94	2.0
2	50.	2.5	0.32	6.56	4.17 (20)	6.68	2.0
3	∞	2.5	0.32	1.31	3.37 (17)	6.70	2.0
R_{e0}=4.59, m=1.6, f_b fitted.							
1	∞	8.0	0.06	2.24	8.29 (25)	10.85	1.65
2	50.	5.0	0.13	6.00	5.39 (20)	9.26	1.36
3	∞	5.5	0.11	0.84	4.15 (17)	9.37	1.45
R_{e0}=5.44, m=2.2, f_b fitted.							
1	∞	6.5	0.07	2.05	6.21 (25)	7.99	1.78
2	50.	3.7	0.16	6.22	4.09 (20)	6.78	1.47
3	∞	5.0	0.10	0.76	3.31 (17)	7.32	1.66

(1) mass within the farthest bin, whose mean distance in kpc is in parentheses.
(2) mass within 30 kpc.

3.1.1. Using the assumptions and data adopted by KHS

The computations carried out using the *KHS* sample and their adopted projected density profile for the cluster system can be considered to be a sort of consistency check with the model considered by *KHS*.

In fact, if we assume $f_b = 1$ (which implies $M_b = 2 \times 10^{10} M_\odot$ as adopted by *KHS*) and the cluster projected profile they adopted (two $R^{1/4}$–laws with scale length 7.2 kpc outside a galactocentric distance of 5 kpc, and 12.5 kpc inside that radius, see their Sect. III), we get a plausible fit for a distribution of the orbits which is essentially isotropic ($r_a/r_{ch} \simeq 70$), a value of $r_{ch} \sim 0.7$ kpc, and total halo mass $\sim 3.8 \times 10^{11} M\odot$ as adopted with the *KHS* model III based on the rotation curve.

Actually, the "optimal" solution from the $\chi^2 - test$ yields with these inputs a solution having ($r_a/r_{ch} \simeq 7$), a value of $r_{ch} \sim 1.3$ kpc, and total halo mass $\sim 4.1 \times 10^{11} M\odot$. We have also examined the possible influence of a different binning of the data in the measure of the projected velocity dispersion, getting the direct evidence that the bulk of the conclusions are unaffected.

This first result ensures that our adopted procedure, though limited to a very specific case, is not inconsistent with the framework obtained by the similar previous study using the same input data.

3.1.2. Using the present sample and the $R^{1/4}$ projected density profile which best fits the data

If we adopt our own sample and compute the best fitting cluster projected density profile imposing the validity of a de Vaucouleurs law, we get a new description of the M 31 cluster system which can be used in the above procedure to get new estimates of the various quantities. To give a direct feeling of the influence of each assumption, we report in Table 3a,b a summary of the results obtained for three different cases and assuming three different binnings. To allow comparisons with the results got above with the *KHS* sample, we have kept here $f_b = 1$.

In the first case, we have included in the fit all the available clusters. Since, as repeatedly noticed, fewer inner clusters have been observed spectroscopically, the fitted effective radius is large and the overall distribution is flat. In the second case, we have excluded from the fit the very central region (r < 0.5 kpc). The fitted effective radius decreases to 5.34 kpc, a value very close to that we obtained in Battistini et al. (1993) from the study of the best adopted sample (supposed to be the least biased).

As can be seen from Table 3a, the results are quite independent of the various assumptions and even of rebinning, yielding substantially the following indications: r_a/r_{ch} is very high (> 70), $r_{ch} \sim 1.1$–1.3 kpc, and the total halo mass increases up to $\sim 5 \times 10^{11} M\odot$ at a distance of 30 kpc, with a fair quality of the fits.

Though limited by the many assumptions, this result seems to show consistently that the addition of the 21 clusters in the outer bins we made compared to the *KHS* sample leads to estimate a larger M 31 halo mass, increasing with increasing the galactocentric distance.

3.1.3. Using the $R^{1/m}$ projected density profile by Battistini et al. 1993

In our previous study (Battistini et al. 1993) we showed that the observed M 31 cluster projected density profile can be probably better fitted by a description a bit different from the "usual" de Vaucouleurs law. The adoption of a cluster projected density profile not represented strictly by a $R^{1/4}$–law has a strong impact on the results. In fact, keeping $f_b = 1$ and adopting the description reported in Eq.(4) for the adopted best sample by Battistini et al. (1993), both r_{ch} and the total halo mass almost double with respect to assuming the $R^{1/4}$–law (see Table 3b). If, more correctly, one recomputes the best fitting parameters using just the clusters included in the present sample, one would get $m = 2.2$ and effective radius $r_e = 5.44$. Adopting these values, r_a/r_{ch} is still very high (> 70), $r_{ch} \sim 2.5$ kpc, and the total halo mass turns out $\sim 6 \times 10^{11} M\odot$ at a distance of 30 kpc (see Table 3b). Figure 2 reports the best fitting velocity dispersion profiles using different data binnings.

© European Southern Observatory • Provided by the NASA Astrophysics Data System

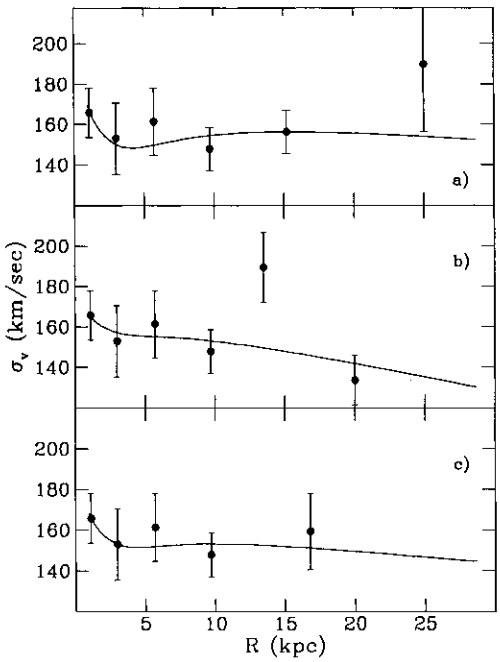

Fig. 2. Plot of the velocity dispersion profile. As can be seen, the best fitting solution varies with varying the binning adopted for the external objects. (a) 60'< R_5 <100', R_6 >100'; (a) 60'< R_5 <80', R_6 >80'; (a) R_5 >60'

Turning now to the more general case described in the procedure where the same inputs are assumed as in the previous case, but leaving f_b to be a free parameter to optimize with the others, we can determine the best set of the f_b, r_a, r_{ch}, ρ_{h0} (and thus M_h, inside the farthest bin or extrapolated to 30 kpc) which yields the best fitting global model.

In synthesis, r_{ch} turns out to be $\sim$ 4–8 kpc, r_a/r_{ch} is always high, $M_b \sim$ 1.3–1.8 $\times 10^{10} M_\odot$, and the total halo mass $\sim$ 6–10$\times 10^{11} M\odot$ at 30 kpc. It is thus easy to see that both the characteristic scale-length and the total halo mass would increase significantly.

How reliable are these estimates? They are strongly model dependent and thus should be taken with particular caution. However, it seems quite proven that the addition of new clusters to the sample of objects with known radial velocities in the outer bins, lead to increase the estimate of the total halo mass. In other words, the velocity dispersion of the new sample in the outer bins is high enough at least to not exclude the presence of a massive halo.

3.2. Using the projected mass method

In order to have further hints and to make comparisons, it may be interesting to apply to the new data–set the "projected mass" (PM) method we already applied in *Paper I* also to re–discuss and stress some important aspects which limitates the effectiveness of the solutions.

Before addressing briefly the status of the application of this method to this specific problem, we notice that this new path will not be totally independent from the previous one as we fixed the constant involved in the PM method equal to 16, and this implies the "a priori" assumption of isotropic cluster orbits as obtained above.

The problems related to the use of *statistical mass estimators*, based on either the *Virial Theorem* (VT) or moments of the PM have been already discussed in *Paper I* (and references therein). However, before going on with the procedure, it is compulsory to stress first again some crucial items related to the problems one has to face when applying such a procedure to the M 31 cluster system and the flaw which in principle affects the use we and others (for instance, van den Bergh 1981; Huchra & Brodie 1987; Huchra et al. 1991) did in the M 31 cluster system.

The PM method as developed by Bahcall & Tremaine (1981) and Heisler et al. (1985) can be straightforwardly used only when one has positions and velocities for a *complete* set of test particles, knowing also their actual orbit distribution, and these requirements are not matched in our specific case.

In order to use anyway this method at least to set some constraints to the M 31 mass, we grouped in *Paper I* the M 31 globular clusters with known radial velocities in distance bins, estimating the mass within each radius with the PM method in the central point mass approximation. The basic ideas underlying this choice were the implicit assumption that the degree of completeness could be taken to be sufficiently independent of galactocentric distance (which we know is not completely true) and the possibility of using the central point mass approximation (which is actually wrong).

As noted by Kent (private communication), these assumptions led us to derive (*Paper I*) masses too high by factors 1.5–2 in the considered radial range. In fact, calculating the circular rotational velocities from the masses given in Table 2 of *Paper I*, one gets figures of about 330–400 km s^{-1}, which are well in excess of the observed HI rotation velocities of about 250 km s^{-1}. On the other hand, due to the poor number of objects at high galactocentric distances, these estimates are subject to quite strong fluctuations enhanced also by the influence of the binning of the data.

The issue of the use of an approach not based on the central point mass approximation is important but not easy to solve. In fact, one could in principle adopt an estimator which could take into accout the mass distribution. However, we would get an estimator depending in a sense on a quantity which should be constrained by the estimator itself.

The results obtained for the radial mass distribution are shown in Table 4. Since the number of clusters in the outer regions is quite low, we have binned the data in two different ways. Consequently, the average galactocentric distance associated to the bin varies. As can be seen, the differences induced by a different grouping of the available data are quite strong. In particular, using the present sample, the total mass could increase up to $\sim 8 \times 10^{11} M_\odot$ if the very outer clusters outside 100 arcmin (7 in total) are binned together. Alternative binnings lead to smaller masses of the order of $\sim 5 \times 10^{11} M_\odot$. Note that even

© European Southern Observatory • Provided by the NASA Astrophysics Data System

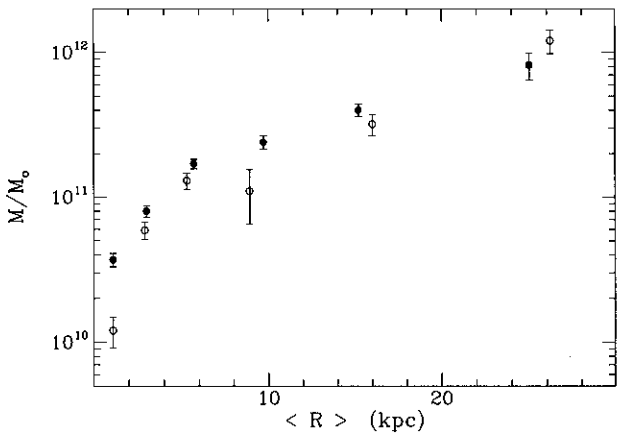

Fig. 3. The M 31 radial mass distribution as obtained by grouping the 176 clusters with known radial velocities in distance bins and estimating the mass within each radius with the *projected mass* method, in the central point mass approximation. The results here got (full dots) are compared with those from *Paper I* (open dots), obtained using 81 clusters

Table 4. Mass determination of M 31 from the present sample obtained via the Projected Mass method

Bin (arcmin)	Projected distance (kpc)	Number of objects	σ_r (km s^{-1})	R (kpc)	Mass (10^{11}M$_\odot$)
0 – 10	0 – 2	27	165.7 ± 12.2	1.1	0.4 ± 0.04
10 – 20	2 – 4	38	153.0 ± 17.6	3.0	0.8 ± 0.1
20 – 40	4 – 8	48	161.3 ± 16.6	5.7	1.7 ± 0.1
40 – 60	8 – 12	28	147.8 ± 10.7	9.7	2.4 ± 0.3
60 –100	12 – 19	31	156.3 ± 10.8	15.2	4.0 ± 0.4
>100	> 19	7	189.8 ± 33.6	25.0	8.2 ± 1.7
60 – 80	12 – 19.5	18	189.4 ± 17.3	13.5	5.3 ± 0.6
> 80	> 15.5	18	133.6 ± 12.2	20.0	4.1 ± 0.6

Notes:
adopted distance 667 kpc;
adopted velocity of the center of mass -301 km s^{-1} (Yahil et al. 1977);
R = average projected radius of the objects in the shell.

this value is about twice as large as that obtained with the same method over the same radial bins but using the *KHS* sample. Hence, we can conclude again that the inclusion of the new data seems to yield a higher value of the estimated mass.

Figure 3 shows the comparison between the present results and those presented in *Paper I* using only 81 clusters.

3.3. The Richstone and Tremaine models (RT): their use in Paper I

In *Paper I*, we used a procedure to fit the observed cluster velocity dispersion, admittedly criticized on a well–grounded basis by the Referee of the present paper.

The basic criticism put forward by Kent consists of two aspects: (1) In *Paper I*, we imposed the only observational constraint that the adopted RT models match the observed velocity dispersion, allowing the two scale parameters for the models (effective radius and total mass) to vary. Since the RT models assume that the ratio of mass to light is constant everywhere and the cluster density profile is known from the data, then the effective radius could not be varied but must be fixed. (2) Our conclusion that the RT model with circular orbits best fits the data we presented in *Paper I* rests on the fundamental implicit assumption that the ratio of halo density to number density of clusters is constant, but this is not assured.

There is no doubt that the point that the "actual" effective radius of the cluster system is known "a priori" independently of the fit is important. Hence, one could carry out some experiments adopting for instance the effective radius, $R_e \sim 4.6$ kpc obtained from the observations of the so-called "best adopted M 31 cluster sample" (Battistini et al. 1993). However, there are two further problems which make hardly significant a re-application of the procedure followed in *Paper I*.

First, the sample of cluster for which the radial velocities are known is smaller than the best adopted sample quoted above. Since it is much easier to get spectra of objects located outside the main body of M 31 itself, there is a small radial selection bias which leads the sample of the spectroscopically measured clusters to yield a slightly larger observed effective radius of 5.44 kpc. The difference is small enough to be probably not very important.

Second, there is an aspect more important which somehow precludes any further step. In fact, the analysis of the cluster projected distribution carried out by Battistini et al. (1993) has shown that the $R^{1/4}$–low could not be the optimal law to use to describe the profile, while its validity is a prerequisite for using the RT-models.

In conclusion, we believe that it would thus be too speculative to proceed along this path until new data and a better knowledge of the cluster projected distribution is available.

4. Final considerations and conclusions

It is quite evident from the analysis reported above that the framework offered by the available data on the M 31 cluster dynamics is still insufficient to properly constrain both the M 31 total mass and its radial distribution. New data on radial velocities of many other clusters (especially in the far halo) are urged and also a precise, radially unbiased description of the cluster projected density profile is necessary to make a correct use of the available galaxy models.

Nevertheless, different procedures applied to the available data-set give some evidence of a steady increase of the M 31 mass up to values typical for the claimed existence of a quite massive halo (~ 5–$8 \times 10^{11} M_\odot$ at 30 kpc). In particular, it seems that, independent of the procedure and the assumptions, the addition of our new data for clusters located in the outer regions leads to increase the estimate of the M 31 total mass previously made using the globular clusters as test particles.

However, we must stress that the assumptions imposed by the methods in absence of a firm knowledge of the cluster actual orbit distribution and of their real spatial description limits quite severely the reliability of this result.

Acknowledgements. The authors want to thank the Academy of Sciences of USSR for kind ospitality during two observing runs at the 6m

© European Southern Observatory • Provided by the NASA Astrophysics Data System

BTA and the SAO staff for the essential help provided during observations. Helpful discussions with P. Battistini are gratefully acknowledged. This research has beeen supported by the *Gruppo Nazionale di Astronomia* of the *Consiglio Nazionale delle Ricerche* and by the *Ministero dell' Università e della Ricerca Scientifica e Tecnologica.* One of us (L.C.) was supported with the NSF Grant AST 9108103.

References

Bahcall, J.N. and Tremaine, S. 1981, ApJ, 244,805.
Battistini, P., Bònoli, F., Braccesi, A., Fusi Pecci, F., Malagnini, M.L., Marano, B. 1980, A&AS, 42, 357
Battistini, P., Bònoli, F., Buonanno, R., Corsi, C.E., and Fusi Pecci, F. 1982, A&A, 113, 39
Battistini, P., Bònoli, F., Braccesi, A., Federici, L., Fusi Pecci, F., Marano, B., Borngen, F. 1987, A&AS, 67, 447 *BoSurvey*
Battistini, P., Bònoli, F., Casavecchia, M., Ciotti, L., Federici, L., Fusi Pecci, F. 1993, A&A, in press
Battistini, P., et al., 1993, in preparation
Binney, J. 1980, MNRAS, 190, 873
Binney, J., Mamon, G.A. 1982, MNRAS, 200, 361
Binney, J., Tremaine, S. 1987, in: Galactic Dynamics, Princeton University Press, Princeton, p.240
Boksenberg, A. 1972, in: ESO/CERN conference on Auxiliary Instrumentation for Large Optical Telescopes, eds. S.Lausten and A.Reiz, p. 295.
Bònoli, F., Delpino, F.E., Federici, L., and Fusi Pecci, F. 1987, A&A, 185, 25
Bònoli, F., Federici, L., and Fusi Pecci, F. 1988, A&A, 205, 6
Bònoli, F., Delpino, F.E., Federici, L., Fusi Pecci, F., and Longmore, A.J. 1992, A&AS, 96, 163
Buonanno, R., Corsi, C.E., Battistini, P., Bònoli, F., Fusi Pecci, F. 1982, A&AS, 47, 451
Cacciari, C., Cassatella, A., Bianchi, L., Fusi Pecci, F., and Kron, R.G. 1982, ApJ, 261, 77
Ciotti, L. 1991 A&A, 249, 99
Cohen, J.G., Freeman, K.C. 1991, AJ, 101, 483
Crotts, A.P.S., Kron, R.G., Cacciari, C., and Fusi Pecci, F. 1990, AJ, 100, 141
Federici, F., Fusi Pecci, F., Marano, B. 1990, A&A, 236, 99 *(Paper I)*
Heisler, J., Tremaine, S., Bahcall, J. 1985, ApJ, 298, 8
Huchra, J., Brodie, J.P. 1987, AJ, 93, 779
Huchra, J., Stauffer, J., and Van Speybroeck, L. 1982, ApJ, 259, L57
Huchra, J.P., Brodie, J.P., Kent, S.M. 1991, ApJ, 370, 495
Kent, S.M. 1987, AJ, 93, 816
Kent, S.M. 1989, AJ, 97, 1614
Kent, S.M., Huchra, J.P.,Stauffer, J. 1989, AJ, 98, 2080 *(KHS)*
Merritt, D. 1985, AJ, 90, 1027
Pier, J.R. 1983, ApJS, 53, 791
Peterson, R. 1989, in: Dynamics of Dense Stellar Systems, ed. D. Merrit, Cambridge, p. 161
Racine, R. 1991, AJ, 101, 865
Richstone,D., Tremaine, S. 1984, ApJ, 286, 27 *(RT)*
Sandage, A.,Tamman, G.A. 1971, ApJ, 167, 293
Sargent, W.L.W., Kowal, C.T., Hartwick, F.D.A., van den Bergh, S. 1977, AJ, 82, 947
Sharov, A.S., Lyutyi, V.M. 1989, SvA, 33,235
Sitko, M.L. 1984, ApJ, 286, 209
Somova, T.A., Somov, N.N., Markelov, S.V., Nebelitskii, O.I., Spiridonova, O.I. and Fomenko, A.F. 1982, in: Instrumentation for Astronomy with Large Optical Telescope, C.M.Humphries Ed., p. 283
van den Bergh, S. 1969, ApJS, 19, 145
van den Bergh, S. 1981, PASP, 93, 428
Yahil, A.,Tamman, G.A.,Sandage, A. 1977, ApJ, 217, 903

This article was processed by the author using Springer-Verlag TEX A&A macro package 1992.

© European Southern Observatory • Provided by the NASA Astrophysics Data System